Available online at www.sciencedirect.com

ScienceDirect

Mendeleev Commun., 2021, **31**, 352–355

Mendeleev Communications

First example of peroxosolvate of iodine-containing organic molecule

Andrei V. Churakov,*[a] Aleksei V. Medved'ko,[b] Petr V. Prikhodchenko,[a] Dmitry P. Krut'ko[c] and Sergey Z. Vatsadze*[b]

[a] *N. S. Kurnakov Institute of Inorganic Chemistry, Russian Academy of Sciences, 119991 Moscow, Russian Federation*

[b] *N. D. Zelinsky Institute of Organic Chemistry, Russian Academy of Sciences, 119991 Moscow, Russian Federation. E-mail: zurabych@gmail.com*

[c] *Department of Chemistry, M. V. Lomonosov Moscow State University, 119991 Moscow, Russian Federation*

DOI: 10.1016/j.mencom.2021.05.023

Six new bispidine-based bis-amides containing residues of haloacetic acids were synthesized and characterized by X-ray crystallography. The dissolution of iodine-containing compound in concentrated hydrogen peroxide afforded bispidine peroxosolvate, in which the peroxide molecules participated in two donor hydrogen bonds with carbonyl oxygen atoms of the distinct adjacent organic molecules thus forming cyclic motifs in crystals. This structure is a first example of peroxosolvate of iodine-containing organic molecule.

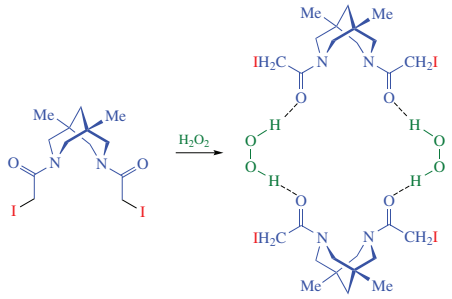

Keywords: 3,7-diazabicyclo[3.3.1]nonane, α-halo carbonyl compounds, hydrogen peroxide, peroxosolvates, organoiodine compounds, conformation analysis, X-ray diffraction study.

Novel forms of drug delivery including controlled release are of great importance nowadays. In particular, co-crystallization of biologically active substance in the form of solvate with appropriate liquid solvent has emerged as a reliable method for modifying the physical properties of active pharmaceutical ingredients (APIs).[1,2] Among those forms, the solvates containing hydrogen peroxide (HP) became extremely popular in recent years[3] since it provides additional antibacterial and hemostatic activities. Although HP is applicable only for external treatment, its solvates seem promising as reliable weight forms of HP. On the other hand, bispidines (3,7-diazabicyclo[3.3.1]nonanes) are the privileged structures in medicinal chemistry.[4] Combination of bispidine-based molecule with HP in the forms of solid solvates looks attractive as it opens the way to making stable forms of biologically active compounds. To the best of our knowledge, none of such structures are documented.

Our general interest in bispidine chemistry lies in the application of such molecules in the synthesis of supramolecular architectures[5] and some macrocycles.[6] We chose the acylation of bispidines as a first step since it proceeds cleaner compared to alkylation. The second step alkylation would furnish the desired macroheterocycle and in general proceeds smoothly due to conformational pre-organization of two halogen atoms, which is typical of bispidines. Additionally, two halogens can be replaced by primary amine function opening a way to a family of AMPA receptor allosteric modulators.[7] The preferable leaving group for nucleophilic substitution is iodine. One should keep in mind that the presence of iodine atoms makes it possible to explore the high potent of I^{III} and I^{V} chemistry. For aliphatic iodides, scarcely reported reagents[8–16] for iodine oxidation gave only I^{III} products. Among the oxidants applied, hydrogen peroxide was not tested; at the same time, amongst 140 peroxosolvate structures deposited in Cambridge Crystallographic Data Centre, aliphatic iodide derivatives were not encountered. Hence, there arises the question: if aliphatic iodides are resistant to hydrogen peroxide, whether new peroxosolvates can be discovered in crystal phase? Alternatively, a new access to valuable hyper-valent iodine-containing bispidine-based building blocks can be developed.

To answer these questions, in this work iodine-containing bispidines were synthesized (Scheme 1), and their solid-state structure and reactivity towards hydrogen peroxide were investigated. Bis(haloacetyl)-containing bispidines **2a**,**b** and **2′a**,**b** were obtained by bridge opening in 5,7-dimethyl-1,3-diazadamantanes **1a**,**b** with the corresponding haloacetyl halides.[17] New iodo derivatives **3a**,**b** were prepared from chlorides **2a**,**b** by the Finkelstein halogen exchange[6] (see Scheme 1).

The behavior of bispidine halides **2**, **3** was initially studied in solutions. As it was mentioned in literature,[6,18] the presence of two amide functions in close proximity in the bispidine leads to the formation of several stereoisomeric forms for compound **2b**, namely, the *dl*-pair whose two carbonyl oxygens exist in *anti*-

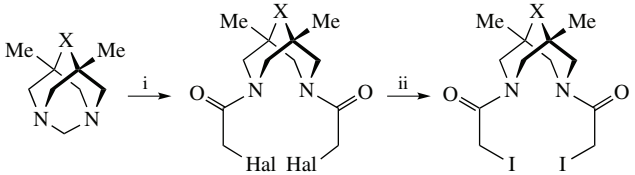

1a X = CO
1b X = CH_2

2a X = CO, Hal = Cl (45%)
2b X = CH_2, Hal = Cl (54%)
2′a X = CO, Hal = Br (52%)
2′b X = CH_2, Hal = Br (50%)

3a X = CO (89%)
3b X = CH_2 (85%)

Scheme 1 *Reagents and conditions*: i, $HalCH_2C(O)Hal$, $NaHCO_3$, PhH, H_2O; ii, NaI, acetone, reflux.

position (C_2 axis of symmetry, see Scheme S1 in Online Supplementary Materials), and the *meso*-form with these two atoms in *syn*-position (plane of symmetry). The *anti*-isomer possesses lower dipole moment compared to that of *syn*-isomer. To answer a question whether the nature of a halogen and of a substituent at C^9-atom of the bicycle affects the conformational behavior of halo acetamides **2** and **3**, we studied their NMR spectra in $CDCl_3$ and DMSO-d_6 (see Online Supplementary Materials, Table S1). In a good agreement with published data,[19] dihalo compounds **2** and **3** show the presence of only *anti*-form in non-polar $CDCl_3$, but exhibit the pronounced signals of *syn*-isomer in more polar DMSO-d_6. At the same time, in this study we revealed that *syn*/*anti* ratios for bis-amides **2** and **3** in DMSO-d_6 depended on the nature of both halogen and substituent at atom C^9, namely, molecules with CH_2 groups prefer *syn*-configuration compared to carbonyl analogues (see Table S1). The origins of this effect as well as the mechanism of amide inversion in bispidine-based bis-amides are a subject of our current investigation. It should be noted that not only *syn*/*anti*-configuration affects the overall dipole moment of molecules **2** and **3**, but also the conformation of halogen substituent in respect to N–C(O)–CH_2 fragment.

Crystal structures in solid states of iodomethyl-substituted bispidin-9-one **3a**, bispidine **3b**, bispidine peroxosolvate **3b**·H_2O_2, bromomethyl-substituted bispidin-9-one **2′a**, and bromomethyl-substituted bispidine **2′b** were determined by X-ray diffractometry† (see also Table S2 in Online Supplementary Materials). The asymmetric units for **3a**, **3b**, **3b**·H_2O_2, **2′a**, and **2′b** are shown in Figures 1, 2, selected bond lengths and angles are presented in Table S2. In all four structures, the molecules occupy general positions; **3b**·H_2O_2 contains two crystallographycally independent bispidines with close geometrical parameters. All bond lengths are ordinary for

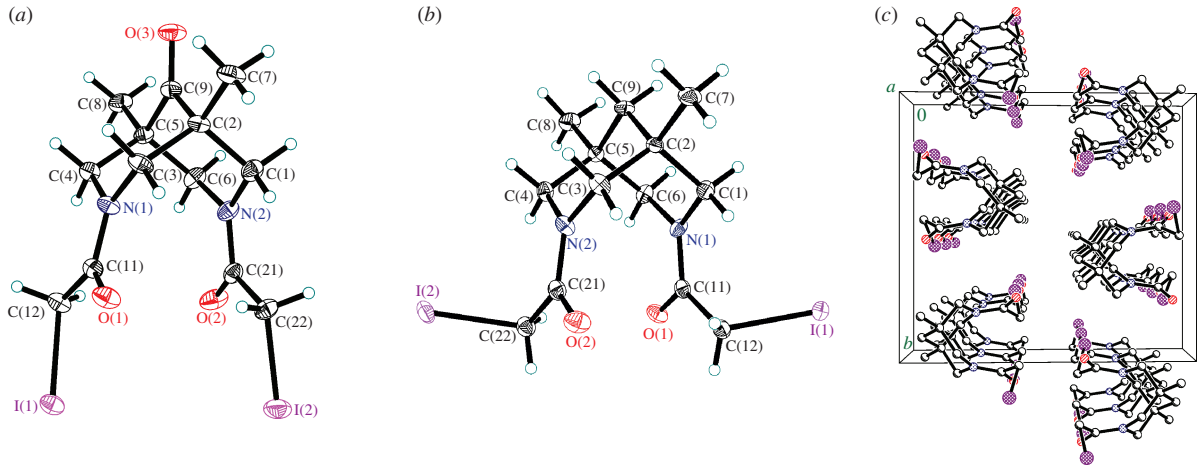

Figure 1 Molecular structures of (*a*) diiodide **3a**, (*b*) diiodide **3b**, and (*c*) crystal packing in the structure **3b**. Displacement ellipsoids are drawn at 50% probability level.

† *Crystal data for* **3a**. $C_{13}H_{18}I_2N_2O_3$, $F_w = 504.09$, triclinic, $a = 8.0984(2)$, $b = 9.9494(3)$ and $c = 11.3056(3)$ Å, $\alpha = 66.5477(9)$, $\beta = 69.4791(8)$ and $\gamma = 77.5030(9)°$, $V = 779.52(4)$ Å^3, space group $P\bar{1}$, $Z = 2$, $D_c = 2.148$ g cm^{-3}, $F(000) = 480$, $\mu(MoK_\alpha) = 4.043$ mm^{-1}, colourless prism with dimensions *ca.* 0.30×0.20×0.15. Total of 12934 reflections (4527 unique, $R_{int} = 0.0235$) were measured on a Bruker D8 Venture diffractometer (graphite monochromatized MoK_α radiation, $\lambda = 0.71073$ Å) using ω-scan mode at 150 K. The final residuals were: $R_1 = 0.0211$ for 4074 reflections with $I > 2\sigma(I)$ and $wR_2 = 0.0460$ for all data and 254 parameters. GoF = 1.038.

Crystal data for **3b**. $C_{13}H_{20}I_2N_2O_2$, $F_w = 490.11$, monoclinic, $a = 7.7120(2)$, $b = 13.6081(3)$ and $c = 15.0465(4)$ Å, $\beta = 93.6593(9)°$, $V = 1575.85(7)$ Å^3, space group $P2_1/c$, $Z = 4$, $D_c = 2.066$ g cm^{-3}, $F(000) = 936$, $\mu(MoK_\alpha) = 3.992$ mm^{-1}, colourless plate with dimensions *ca.* 0.45×0.40×0.10. Total of 18684 reflections (4569 unique, $R_{int} = 0.0234$) were measured on a Bruker SMART APEX II machine (graphite monochromatized MoK_α radiation, $\lambda = 0.71073$ Å) using ω-scan mode at 100 K. The final residuals were: $R_1 = 0.0242$ for 4341 reflections with $I > 2\sigma(I)$ and $wR_2 = 0.0519$ for all data and 252 parameters. GoF = 1.224.

Crystal data for **3b**·H_2O_2. $C_{13}H_{22}I_2N_2O_4$, $F_w = 524.12$, triclinic, $a = 7.7873(3)$, $b = 13.9039(6)$ and $c = 16.1367(7)$ Å, $\alpha = 90.5863(15)$, $\beta = 92.0803(15)$ and $\gamma = 99.9612(14)°$, $V = 1719.47(12)$ Å^3, space group $P\bar{1}$, $Z = 4$, $D_c = 2.025$ g cm^{-3}, $F(000) = 1008$, $\mu(MoK_\alpha) = 3.674$ mm^{-1}, colourless needle with dimensions *ca.* 0.50×0.10×0.02. Total of 25807 reflections (7471 unique, $R_{int} = 0.0293$) were measured on a Bruker SMART APEX II machine (graphite monochromatized MoK_α radiation, $\lambda = 0.71073$ Å) using ω-scan mode at 150 K. The final residuals were: $R_1 = 0.0282$ for 6711 reflections with $I > 2\sigma(I)$ and $wR_2 = 0.0581$ for all data and 422 parameters. GoF = 1.104.

Crystal data for **2′a**. $C_{13}H_{18}Br_2N_2O_3$, $F_w = 410.11$, monoclinic, $a = 8.111(3)$, $b = 20.818(8)$ and $c = 9.245(2)$ Å, $\beta = 90.71(3)°$, $V = 1560.9(9)$ Å^3, space group $P2_1/n$, $Z = 4$, $D_c = 1.745$ g cm^{-3}, $F(000) = 816$, $\mu(MoK_\alpha) = 5.201$ mm^{-1}, colourless prism with dimensions *ca.* 0.30×0.25×0.20. Total of 4907 reflections (3054 unique, $R_{int} = 0.0386$) were measured on an Enraf-Nonius CAD4 diffractometer (graphite monochromatized MoK_α radiation, $\lambda = 0.71073$ Å) using ω-scan mode at 295 K. The final residuals were: $R_1 = 0.0597$ for 1461 reflections with $I > 2\sigma(I)$ and $wR_2 = 0.2233$ for all data and 183 parameters. GoF = 1.015.

Crystal data for **2′b**. $C_{13}H_{20}Br_2N_2O_2$, $F_w = 396.13$, monoclinic, $a = 7.7677(3)$, $b = 19.8219(7)$ and $c = 9.7022(3)$ Å, $\beta = 103.038(1)°$, $V = 1455.34(9)$ Å^3, space group $P2_1/c$, $Z = 4$, $D_c = 1.808$ g cm^{-3}, $F(000) = 792$, $\mu(MoK_\alpha) = 5.570$ mm^{-1}, colourless prism with dimensions *ca.* 0.20×0.20×0.08 mm. Total of 13694 reflections (3518 unique, $R_{int} = 0.0279$) were measured on a Bruker D8 Venture diffractometer (graphite monochromatized MoK_α radiation, $\lambda = 0.71073$ Å) using ω-scan mode at 150 K. The final residuals were: $R_1 = 0.0212$ for 3050 reflections with $I > 2\sigma(I)$ and $wR_2 = 0.0473$ for all data and 252 parameters. GoF = 1.031.

The structures were solved by direct methods and refined by full matrix least-squares on F^2 with anisotropic thermal parameters for all non-hydrogen atoms.[25] In the structure **3b**·H_2O_2, one of the two crystallographically independent peroxide molecules is cross-type disordered over two positions with occupancy ratio 0.60(1)/0.40(1). In **3a** and **3b**, all hydrogen atoms were found from difference Fourier synthesis and refined with isotropic thermal parameters. In **3b**·H_2O_2, all carbon H atoms were placed in calculated positions and refined using a riding model, while peroxide H atoms were localized objectively, and their positional parameters were refined with restrained O–H distances (SADI). As for **2′a**, all hydrogen atoms were placed in calculated positions and refined using a riding model.

CCDC 2048266–2048268, 2049144, and 1860309 contain the supplementary crystallographic data for this paper. These data can be obtained free of charge from The Cambridge Crystallographic Data Centre *via* http://www.ccdc.cam.ac.uk.

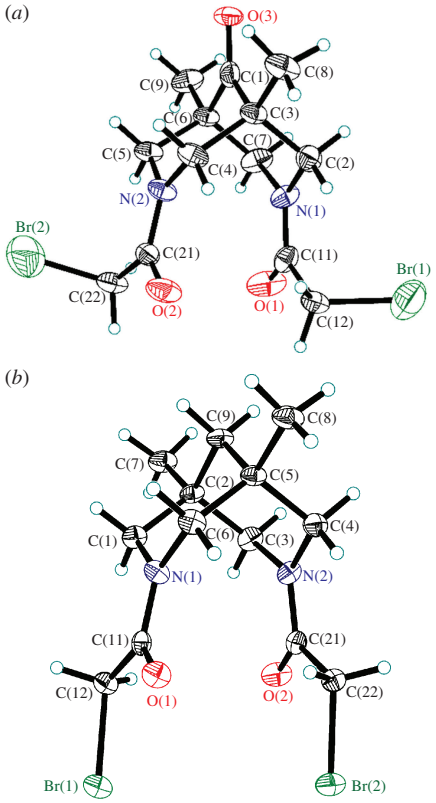

Figure 2 Molecular structures of (*a*) dibromide **2′a** and (*b*) dibromide **2′b**. Displacement ellipsoids are drawn at 50% probability level.

organic compounds.[20] In all cases bispidine core adopts the most typical chair–chair conformation[21] with noticeably shortened intermolecular N···N separations [2.805(3)–2.834(4) Å]. Amide fragments R_2N–C(=O)–C are planar within 0.08 Å.

In these structures, the conformation of O=C–C–I groups attracts particular interest. In **3a**, these groups are almost planar; in **3b** and **3b** · H_2O_2, the corresponding torsion angles are close to 90°. According to Cambridge Structural Database, the 'perpendicular' conformation is preferable for acyclic R_2NC(=O)–C–I and R_2NC(=O)–C–Br fragments (Figures S1 and S2, Online Supplementary Materials). Surprisingly, the distribution for chlorine analogues is opposite (Figure S3). Of interest, C–I distances in **3a** are slightly shorter (~0.03 Å) than in **3b** and **3b** · H_2O_2.

The structure **3b** · H_2O_2 contains two crystallographycally independent hydrogen peroxide molecules (Figure 3). The O–O distances vary within 1.455(13)–1.462(9) Å values that are close to the mean O–O bond length (1.45 Å) for solvent H_2O_2 molecules deposited in Cambridge Structural Database (78 entries). Peroxide molecules adopt skew conformations with H–O–O–H torsion angles ranging within 97(5)–118(10)°. One of peroxide molecules is cross-type disordered. Both components of the disorder are H-bonded with the same carbonyl oxygen atoms of neighboring organic conformers. Hydrogen peroxide disorder of this sort is well-known for organic peroxosolvates.[22,23] As expected, peroxide molecules in **3b** · H_2O_2 form only two donor hydrogen bonds since organic counterpart does not contain reasonable hydrogen bond donor.[24] On other side, **3b** · H_2O_2 is the rare example of hydrogen bonding between hydrogen peroxide and amide groups.[23] In crystal, H_2O_2 molecules serve as supramolecular linkers between adjacent organic molecules [see Figure 3(*b*)]. Despite the high content of iodine, in molecules **3a** and **3b** · H_2O_2 only one for each structure short intermolecular I···I contacts is observed (3.87 and 3.94 Å, respectively). Moreover, in **3b** there are no short I···I contacts at all [see Figure 1(*c*)]. To

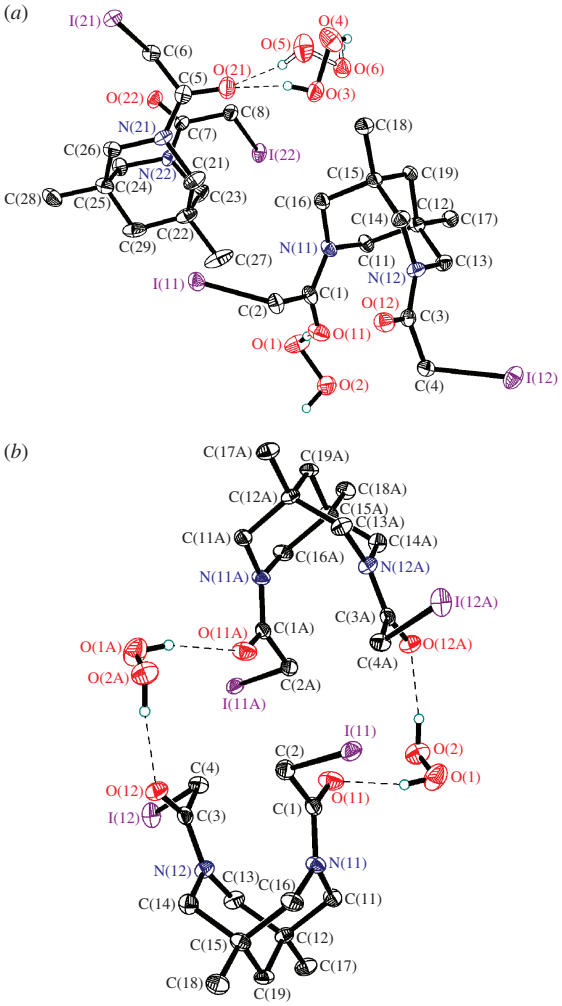

Figure 3 Molecular structure of (*a*) **3b** · H_2O_2, minor component of disordered peroxide molecule is shown by open lines, and (*b*) centrosymmetric peroxide-bonded dimers in the structure **3b** · H_2O_2. Hydrogen bonds are shown by dashed lines. Displacement ellipsoids are drawn at 50% probability level.

the best of our knowledge, compound **3b** · H_2O_2 is the first example of iodine-containing peroxosolvate.

In conclusion, we have revealed the possibility of formation of stable crystalline peroxosolvates with organoiodine compounds.

Synthesis and structure determination of peroxosolvate **3b** · H_2O_2 were performed under the program of Russian Foundation for Basic Research (grant no. 20-03-00449). X-ray studies were carried out at the Centre of Shared Equipment of the N. S. Kurnakov Institute of General and Inorganic Chemistry, Russian Academy of Sciences. The authors thank Dr. P. Postnikov and Ms. Yu. Vlasenko (Tomsk Polytechnical University) for helpful discussion.

Online Supplementary Materials

Supplementary data associated with this article can be found in the online version at doi: 10.1016/j.mencom.2021.05.023.

References

1 G. Bolla and A. Nangia, *Chem. Commun.*, 2016, **52**, 8342.
2 R. Hilfiker, F. Blatter and M. von Raumer, in *Polymorphism: in the Pharmaceutical Industry*, ed. R. Hilfiker, Wiley-VCH, 2006, pp. 1–19.
3 K. M. Kersten, M. E. Breen, A. K. Mapp and A. J. Matzger, *Chem. Commun.*, 2018, **54**, 9286.
4 I. Tomassoli, D. Gündisch and D. Guendisch, *Curr. Top. Med. Chem.*, 2016, **16**, 1314.

5 S. Z. Vatsadze, A. V. Medved'ko, A. A. Bodunov and K. A. Lyssenko, *Mendeleev Commun.*, 2020, **30**, 344.
6 S. Z. Vatsadze, D. P. Krut'ko, A. J. Blake and P. Mountford, *Macroheterocycles*, 2017, **10**, 98.
7 M. I. Lavrov, P. N. Veremeeva, D. S. Karlov, V. L. Zamoyski, V. V. Grigoriev and V. A. Palyulin, *Mendeleev Commun.*, 2019, **29**, 619.
8 V. Montanari, D. D. DesMarteau and W. T. Pennington, *J. Mol. Struct.*, 2000, **550–551**, 337.
9 V. V. Zhdankin and C. Kuehl, *Tetrahedron Lett.*, 1994, **35**, 1809.
10 T. Mukherjee, S. Biswas, A. Ehnbom, S. K. Ghosh, I. El-Zoghbi, N. Bhuvanesh, H. S. Bazzi and J. A. Gladysz, *Beilstein J. Org. Chem.*, 2017, **13**, 2486.
11 T. Kawashima, K. Hoshiba and N. Kano, *J. Am. Chem. Soc.*, 2001, **123**, 1507.
12 V. V. Zhdankin, C. J. Kuehl and A. J. Simonsen, *Tetrahedron Lett.*, 1995, **36**, 2203.
13 V. V. Zhdankin, C. J. Kuehl and A. J. Simonsen, *J. Org. Chem.*, 1996, **61**, 8272.
14 A. A. Zagulyaeva, M. S. Yusubov and V. V. Zhdankin, *J. Org. Chem.*, 2010, **75**, 2119.
15 G. Asensio, C. Andreu, C. Boix-Bernardini, R. Mello and M. E. González-Nuñez, *Org. Lett.*, 1999, **1**, 2125.
16 D. Nicoletti, A. A. Ghini and G. Burton, *J. Org. Chem.*, 1996, **61**, 6673.
17 A. V. Medved'ko, B. V Egorova, A. A. Komarova, R. D. Rakhimov, D. P. Krut'ko, S. N. Kalmykov and S. Z. Vatsadze, *ACS Omega*, 2016, **1**, 854.
18 P. N. Veremeeva, I. V. Grishina, O. V. Zaborova, A. D. Averin and V. A. Palyulin, *Tetrahedron*, 2019, **75**, 4444.
19 Z. Wang, M. J. Islam, V. N. Vukotic and M. J. Revington, *J. Org. Chem.*, 2016, **81**, 2981.
20 C. R. Groom, I. J. Bruno, M. P. Lightfoot and S. C. Ward, *Acta Crystallogr.*, 2016, **B72**, 171.
21 A. V. Medved'ko, A. I. Dalinger, V. N. Nuriev, V. S. Semashko, A. V. Filatov, A. A. Ezhov, A. V. Churakov, J. A. K. Howard, A. A. Shiryaev, A. E. Baranchikov, V. K. Ivanov and S. Z. Vatsadze, *Nanomaterials*, 2019, **9**, 89.
22 D. A. Grishanov, M. A. Navasardyan, A. G. Medvedev, O. Lev, P. V. Prikhodchenko and A. V. Churakov, *Angew. Chem., Int. Ed.*, 2017, **56**, 15241.
23 A. V. Churakov, D. A. Grishanov, A. G. Medvedev, A. A. Mikhaylov, T. A. Tripol'skaya, M. V. Vener, M. A. Navasardyan, O. Lev and P. V. Prikhodchenko, *CrystEngComm*, 2019, **21**, 4961.
24 I. Yu. Chernyshov, M. V. Vener, P. V. Prikhodchenko, A. G. Medvedev, O. Lev and A. V. Churakov, *Cryst. Growth Des.*, 2017, **17**, 214.
25 G. M. Sheldrick, *Acta Crystallogr.*, 2008, **A64**, 112.

Received: 10th December 2020; Com. 20/6391